GEOLOGICA CARPATHICA, 50, 3, BRATISLAVA, JUNE 1999
229–239

SILURIAN–DEVONIAN $^{40}Ar/^{39}Ar$ MINERAL AGES FROM THE KAINTALECK NAPPE: EVIDENCE FOR MID-PALEOZOIC TECTONOTHERMAL ACTIVITY IN UPPER AUSTROALPINE BASEMENT UNITS OF THE EASTERN ALPS (AUSTRIA)

ROBERT HANDLER[1], FRANZ NEUBAUER[1], SIEGFRIED HERMANN[2] and R. DAVID DALLMEYER[3]

[1]Department of Geology and Paleontology, University of Salzburg, Hellbrunner Str. 34, 5020 Salzburg, Austria; robert.handler@sbg.ac.at
[2]Department of Geology and Paleontology, University Graz, Heinrichstr. 26, 8010 Graz, Austria
[3]Department of Geology, University Georgia, Athens, Ga 30602, U.S.A.

(Manuscript received May 11, 1998; accepted in revised form December 9, 1998)

Abstract: $^{40}Ar/^{39}Ar$ mineral dating has been carried out within the amphibolite-facies metamorphic basement and greenschist-facies metamorphic cover of various tectonic units within the Kaintaleck Nappe, Eastern Alps, Austria, to evaluate the age of pre-Alpine metamorphism. Hornblendes display discordant $^{40}Ar/^{39}Ar$ apparent age spectra, minimum ages recorded in medium- to high-temperature gas release steps are ca. 430–405 Ma. White mica from micaschist record discordant $^{40}Ar/^{39}Ar$ age spectra with ages of ca. 350–379 Ma in medium- and high-temperature increments. White mica from discordant aplite and pegmatite record $^{40}Ar/^{39}Ar$ plateau ages of 375.4 ± 0.4 Ma and 364.0 ± 0.8 Ma respectively. The new isotopic ages indicate that (1) mid-Paleozoic (e.g. 430–380 Ma) tectonometamorphic activity is recorded within the basement of the Kaintaleck Nappe; (2) this basement cannot represent the metamorphic basement for Ordovician to Late-Cretaceous sedimentary sequences of the Noric-Tirolic nappe complex (within uppermost units of the Austroalpine nappe complex); (3) the tectonometamorphic evolution of this basement unit contrasts with that of other basement units exposed in the Eastern Alps, where predominantly "late Variscan" (e.g. 330–300 Ma) tectonometamorphic events are recorded in Silurian to Early Carboniferous passive continental margin sequences; and therefore (4) at least two contrasting terranes comprise the Austroalpine basement.

Key words: Eastern Alps, Austroalpine, basement, mid-Paleozoic, terranes, $^{40}Ar/^{39}Ar$, geochronology.

Regional geologic setting

Mesozoic convergence between African-/Adriatic-derived and Eurasian continental elements resulted in subduction of oceanic crust and terminated with continent-continent collision resulting in formation of the Alpine-Carpathian orogen (Frisch 1979; Coward & Dietrich 1989; Dewey et al. 1989). The overall tectonic evolution of the Eastern Alps has been described by Frank (1987) and Tollman (1987). The Eastern Alps of Austria are dominated by nappe complexes, which were initiated within northern sectors of the African/Adriatic realm south of the Jurassic Penninic oceanic realm. These nappes have been collectively termed the Austroalpine nappe complex. Initial Alpine metamorphism and nappe assembly within this nappe complex occurred between ca. 120 and 70 Ma (see Frank et al. 1987 for a compilation of geochronological data), and was contemporaneous to the closure of remnants of the Tethys oceanic realm, which was situated south of the Penninic ocean (Thöni & Jagoutz 1993; Dallmeyer et al. 1998). From footwall to hangingwall the Austroalpine nappe complex may be described in terms of three regional, internally imbricated, tectonic units (Fig. 1), which include the Lower, Middle, and Upper Austroalpine nappe complexes (Tolmann 1963, 1987).

Recent mapping and structural investigations within the northeastern sectors of the Upper Austroalpine nappe complex documented evidence for five Alpine nappes (Figs. 1, 2) which include, from footwall to hangingwall, the Veitsch, Silbersberg, Kaintaleck, Noric-Tirolic, and Juvavic nappes (see Neubauer et al. 1994 for a more detailed description of the stratigraphy). The age of nappe assembly is constrained by Permian cover sequences which form hangingwall segments of the Veitsch, Silbersberg, and Noric-Tirolic nappe complexes. $^{40}Ar/^{39}Ar$ muscovite and whole-rock ages from penetratively ductile deformed sequences of the Upper Austroalpine nappe complex indicate that nappe assembly occurred at 100–90 Ma (Dallmeyer et al. 1996, 1998) and was contemporaneous with regional, sub- to lower greenschist-facies metamorphism within hangingwall units (Frank et al. 1987; Kralik et al. 1987). Within the lowermost Veitsch Nappe and the uppermost Juvavic Nappe only post-Variscan cover sequences (Late Paleozoic and Mesozoic respectively) are recorded. The Silbersberg and Noric-Tirolic nappes consist of Paleozoic lower greenschist-facies metamorphic basement sequences and Permian to Mesozoic cover sequences. Only within the Kaintaleck Nappe, an amphibolite-facies metamorphic basement is recorded, which is overlain by a greenschist-facies metamorphic cover sequence, for which a Late Devonian to Early Carboniferous ages have been suggested (Handler et al. 1997). The preservation of pre-Alpine $^{40}Ar/^{39}Ar$ plateau ages in detrital white mica of various clastic units within the Veitsch, Silbersberg and Noric-Tirolic nappe complexes, indicates that the pre-Alpine K-Ar isotopic system was not significantly rejuvenated within the Upper

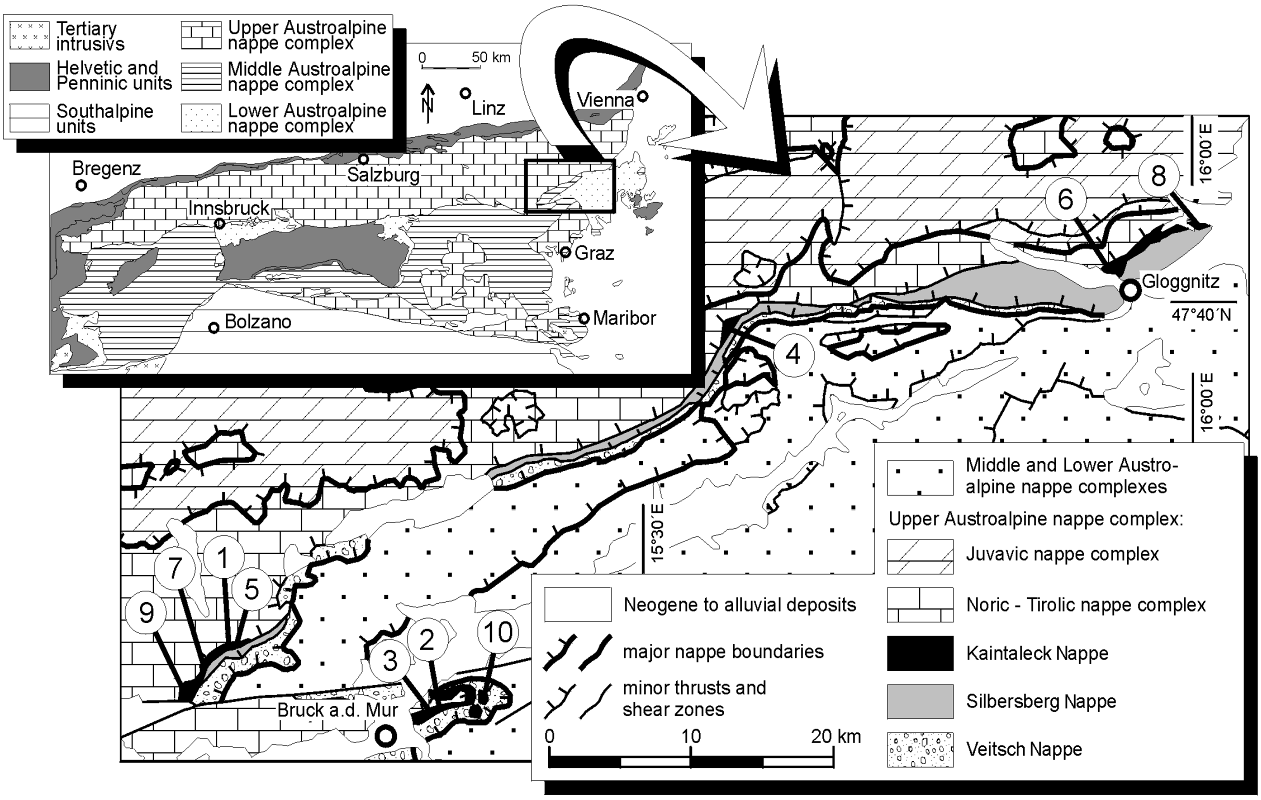

Fig. 1. Geological map of the eastern part of the Eastern Alps. Position of sample localities and sample numbers are indicated.

Austroalpine nappe complex during Alpine tectonothermal activity (Handler et al. 1997).

Tectonic significance of the Kaintaleck Nappe

The basement of the Kaintaleck Nappe (e.g. Kaintaleck Metamorphic Complex; Neubauer et al. 1994) comprises several tectonic basement units which are imbricated between the Silbersberg and the Noric-Tirolic nappes. The Kaintaleck Nappe can be traced over more than 100 km along northeastern sectors of the Eastern Alps (Fig. 1). Rocks comprising the Kaintaleck Metamorphic Complex include amphibolite-facies metamorphic micaschits, marbles and retrogressed eclogite-facies metamorphic amphibolites which were intruted by discordant pegmatite and aplite following initial metamorphism and deformation. At least one of these basement units is unconformably overlain by a meta-conglomerate which was deformed and metamorphosed under greenschist-facies metamorphic conditions (Neubauer 1985). The foliation within the meta-conglomerate clearly transects a pre-existing foliation within underlying amphibolite. This relationship indicates that this meta-conglomerate represents a cover sequence of the Kaintaleck Metamorphic Complex (Neubauer et al. 1987). This meta-conglomerate has been correlated with the Kalwang Conglomerate exposed in a comparable tectonic position westward (Daurer & Schönlaub 1987; Loeschke et al. 1990). Because of its position at the base of fossil-bearing, low-grade metamorphic early Paleozoic clastic sequences of the Noric-Tirolic nappe complex, these authors suggested a late Ordovician age for sedimentation, and subsequent workers (Frisch et al. 1984; Neubauer et al. 1987) have interpreted the Kaintaleck Metamorphic Complex to represent possible remnants of a pre-late Ordovician basement of the Noric-Tirolic nappe complex, although several ductile shear zones have been locally described between the conglomerate and overlying fossil-bearing clastic and carbonatic sequences (Loeschke et al. 1990). On the basis of ^{40}Ar/^{39}Ar dating of detrital white mica for provenance analyses and paleogeographic reconstructions, Handler et al. (1997) suggested a Late Devonian–Early Carboniferous age for the deposition of the Kalwang Conglomerate.

Geochronological evidence for a late Cambrian (e.g. 520–500 Ma) record within the Kaintaleck Metamorphic Complex includes U-Pb zircon data (Neubauer & Frisch 1993) for two orthogneiss-boulders of the transgressive meta-conglomerate (upper intercept ages ca. 500 Ma), and underlying garnet-gneiss intercalated within amphibolite (lower intercept age ca. 516 Ma). However, additional U-Pb zircon data from other units within the Kaintaleck Metamorphic Complex (Neubauer & Frisch 1993) suggest a mid-Paleozoic (e.g. 400–360 Ma) age for the amphibolite-facies tectonothermal event recorded within this basement unit. A record of Caledonian tectonothermal activity markedly contrasts with the pre-Alpine evolution defined for other basement units exposed in the Eastern Alps which were predominantly affected by Cambrian-Ordovician (e.g. 550–440 Ma) and late Variscan (e.g. 330–300 Ma) tectonothermal activity (Frank et al. 1987; Gebauer 1993; Hoinkes & Thöni 1993; Magetti & Flisch 1993; Neubauer & Frisch 1993; Schulz et al. 1993; Spillmann & Büchi 1993).

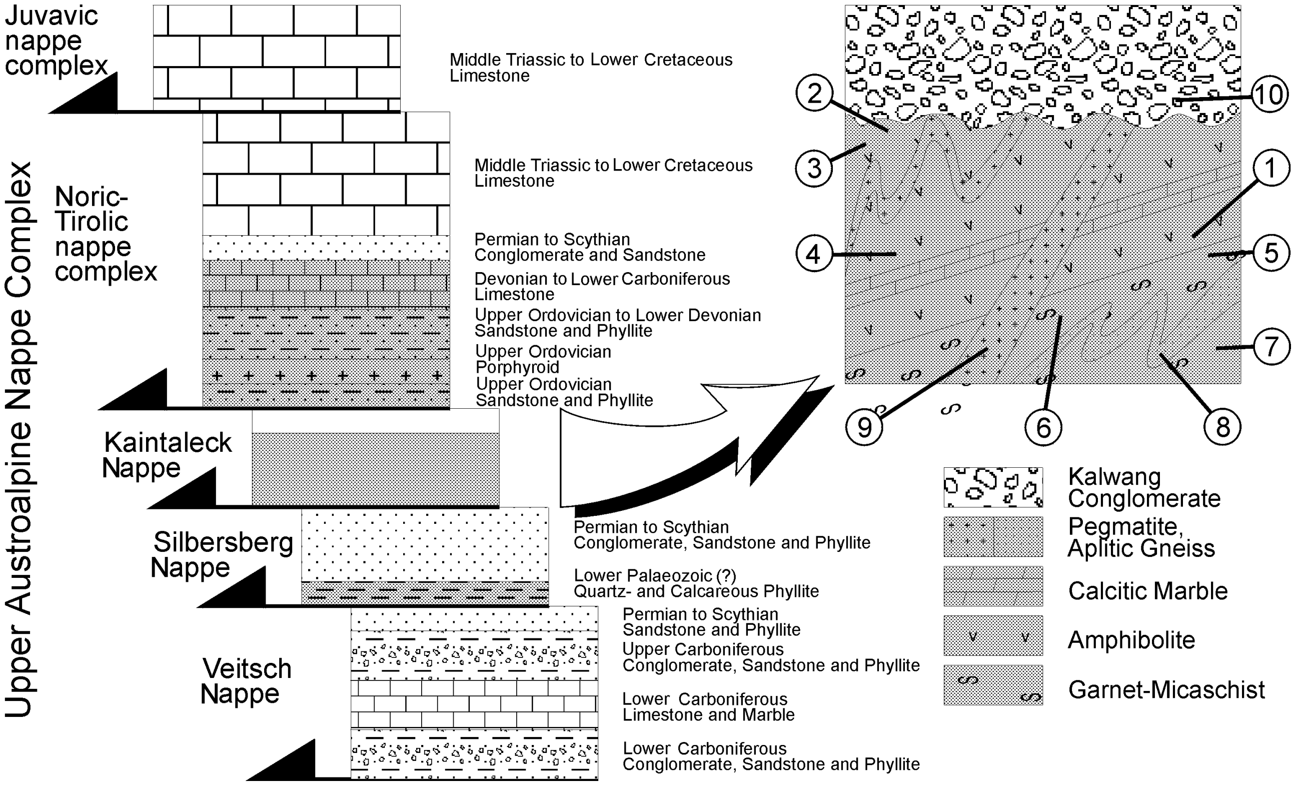

Fig. 2. Schematic tectonostratigraphic profile of eastern sectors of the Upper Austroalpine nappe complex and simplified sketch of the Kaintaleck Nappe indicating sample locations. Hatched areas represent pre-Alpine basement sequences. Thickness of individual nappes is not scaled.

The present study was initiated in an effort to constrain the age of the amphibolite-facies metamorphic tectonothermal activity which affected various tectonic units comprising the Kaintaleck Metamorphic Complex, and to clarify the regional tectonic significance of this crystalline unit within the Austroalpine nappe complex.

Characteristic of the Kaintaleck Metamorphic Complex

Gneisses, garnet-micaschists, and amphibolites reached amphibolite-facies peak metamorphic conditions. Locally, eclogite-facies metamorphic conditions have been described by Neubauer & Frisch (1993). These assemblages were subsequently retrogressed under epidote-amphibolite- and later greenschist-facies metamorphic conditions. All rocks analyzed in the present study display evidence for penetrative ductile deformation under greennschist-facies metamorphic conditions which altered previously formed, amphibolite-facies mineral assemblages. The age of this retrogressive overprint is unclear. However, regional observations and isotopic data from adjacent, over- and underlying, units (Dallmeyer et al. 1996, 1998) argue for an Alpine age for the greenschist-facies metamorphic overprint. The dated minerals represent part of the “older” (amphibolite-facies) parageneses, and are preserved as structural relics, now forming porphyroclasts within a fine-grained matrix of newly grown greenschist-facies retrograde metamorphic minerals.

Within amphibolites, hornblendes have been sheared along crystallographically determined cleavage planes. Plagioclase has been altered to a fine-grained assemblage of white mica and epidote-clinozoisite. Hornblende and plagioclase are surrounded by a fine-grained matrix of chlorite + epidote + clinozoisite + carbonate. A newly-developed penetrative foliation is defined by the orientation of newly-grown chlorite and matrix minerals epidote + (clino-)zoisite + chlorite + carbonate + ore minerals. Within this matrix hornblendes have been oriented parallel to the stretching lineation due to passive, external grain rotation. Because hornblendes acted as rigid clasts during greenschist-facies deformation, it is evident that these minerals represent part of an older, amphibolite-facies metamorphic event.

A similar greenschist-facies metamorphic overprint on an older mineral assemblage is observed within garnet-micaschists. Penetrative ductile deformation resulted in plastic elongation of older quartz grains which are elongated parallel to the stretching lineation and display subgrain formation, core-mantle textures, and syntectonically recrystallized grains. Such features have been described as typical of intracrystalline plastic deformation. Subgrains separated by low-angle grain boundaries (Bell & Etheridge 1973) have been reported to be the result of dislocation glide and climb under conditions of power-law creep (Barber 1985; Langdon 1985). The dominant annealing process for minerals which have been deformed under such conditions has been reported to be syntectonic recrystallization (White 1977; Etheridge & Wilkie 1979, 1981; Gottstein & Mecking 1985). White (1976) describes core-mantle textures as a typical feature for beginning recrystallization along the margins of older deformed grains with high internal strain. According to Sibson (1977, 1980) the fabrics mentioned above require minimum temperatures of ca. 250–300 °C to be rechead during deformation. Quartz grains form elongated aggregates of individual grains which are separated from each other by microcracks and highly curved grain boundaries in some micaschists. Although the overall elongated grain shape would argue for plastic deformation processes, experimental studies (Den Brok 1992) argue for a cataclastic flow regime (Schmidt 1982) for the development of such microstructures.

Within a newly-grown matrix of fine-grained white mica and chlorite, garnet and white mica of the older paragenesis were deformed by cataclastic stretching and external grain rotation parallel to the newly developed stretching lineation. Cracks within garnets are filled with newly-grown chlorite. The micas represent structural relics of an older mineral paragenesis, their rims have partly been recrystallized. Similar passively rotated mica clasts have been termed mica-fish by Lister & Snoke (1984).

Analytical techniques

Sample localities are shown in Figs. 1 and 2. A detailed description of samples and sample localities is provided in the Appendix. Sample preparation procedures are described in Handler (1994).

Mineral concentrates were wrapped in aluminum-foil packets, encapsulated in sealed quartz vials, and irradiated in the US Geological Survey TRIGA reactor. Variations in the flux of neutrons along the lenght of the irradiation assembly were monitored with several mineral standards, including MMhb-1 (Samson & Alexander 1987). Samples were incrementally heated until fusion in a double-vacuum, resistance-heated furnace following procedures described by Dallmeyer & Gil Ibarguchi (1990). Temperatures were monitored with a direct-contact thermocouple and are controlled to ± 1 °C between increments and are accurate to ± 5 °C. Blank-corrected isotopic ratios were adjusted for the effects of mass discrimination and interfering isotopes produced during irradiation using the factors reported by Dalrymple et al. (1981). Apparent $^{40}Ar/^{39}Ar$ ages were calculated from the corrected isotopic ratios using the decay constants and isotopic abundance ratios listed by Steiger & Jäger (1977). Intralaboratory uncertainties are reported, and have been calculated by statistical propagation of uncertainties associated with measurement of each isotopic ratio (at two standard deviations of the mean) through the age equation following the methods described by Dallmeyer & Keppie (1987). A "plateau" is considered defined if ages recorded by four or more contiguous gas fractions (with similar apparent K/Ca rations) each representing more than 5 % of the total ^{39}Ar evolved (and together constituting more than 50 % of the total quantity of ^{39}Ar evolved) are mutually similar within a ± 1 % intralaboratory uncertainty. Plateau ages are calculated by normalizing the appropriate incremental data. Interlaboratory uncertainties are less than ± 1.5 % of the quoted age. Analysis of the MMhb-1 monitor indicates that the apparent K/Ca ratio may be calculated as $0.518\ (\pm 0.005) \times (^{39}Ar/^{37}Ar)_{corrected}$.

Results

Five hornblende concentrates from four amphibolite samples, and six muscovite concentrates from three garnet-mica schist samples, one discordant pegmatite and one aplite sample of the Kaintaleck Metamorphic Complex, and one orthogneiss boulder of the meta-conglomerate overlying the Kaintaleck Metamorphic Complex have been dated by $^{40}Ar/^{39}Ar$ dating technique. Analytical data are listed in Tables 1 and 2, and are portrayed as age spectra in Figs. 3 and 4.

Hornblende

Hornblendes have been collected within three different units of the Kaintaleck Metamorphic Complex. However, they display comparable, internally discordant $^{40}Ar/^{39}Ar$ age spectra (Fig. 3). In low-temperature gas portions they display significant intrasample fluctuations in apparent K/Ca ratios, which suggests experimental release of argon from compositionally distinct, relatively non-retentive phases. In medium- to high-temperature increments apparent ages display either saddle-shape gas release patterns or decreasing stair-case shapes. This may be caused by minor, optically undetectable mineralogical contaminants in the concentrates, petrographically unresolvable exsolution lamellae, compositional zonation of the amphibole grains, or incorporation of an extraneous argon component.

These discordant spectra are interpreted to reflect Alpine and/or pre-Alpine alteration and retrogression of previously formed amphibolites. Apparent ages reported in the age spectra are therefore interpreted as geologically not significant due to probable incorporation of extraneous argon components. However, the youngest ages recorded in medium- and high-temperature gas release steps (430–405 Ma) might be interpreted as the lowermost limits for closure of the K-Ar isotopic system in hornblende subsequent to amphibolite-facies metamorphism.

Muscovite

The results from $^{40}Ar/^{39}Ar$ step heating on white mica concentrates are presented in Fig. 4. Because the apparent K/Ca ratios are very large and exhibit no significant or systematic variations throught the analyses, they are not included in this figure.

$^{40}Ar/^{39}Ar$ age spectra from three white mica concentrates separated from garnet-micaschist samples 5, 6, and 7 are shown in Fig. 4a–c. All $^{40}Ar/^{39}Ar$ age spectra exhibit nearly identical apparent age patterns. The low-temperature portions of the age spectra yield ages ranging between 285 Ma (sample 5) and 200 Ma (sample 6). Intermediate-temperature increments of samples 5 and 7 (Fig. 4a,c) are dominated by apparent ages of 350 Ma. The apparent ages of all samples increase in high-temperature increments to ages ranging between 375 Ma (sample 7) and 379 Ma (sample 6). These stair-case-type gas release spectra have been shown in other

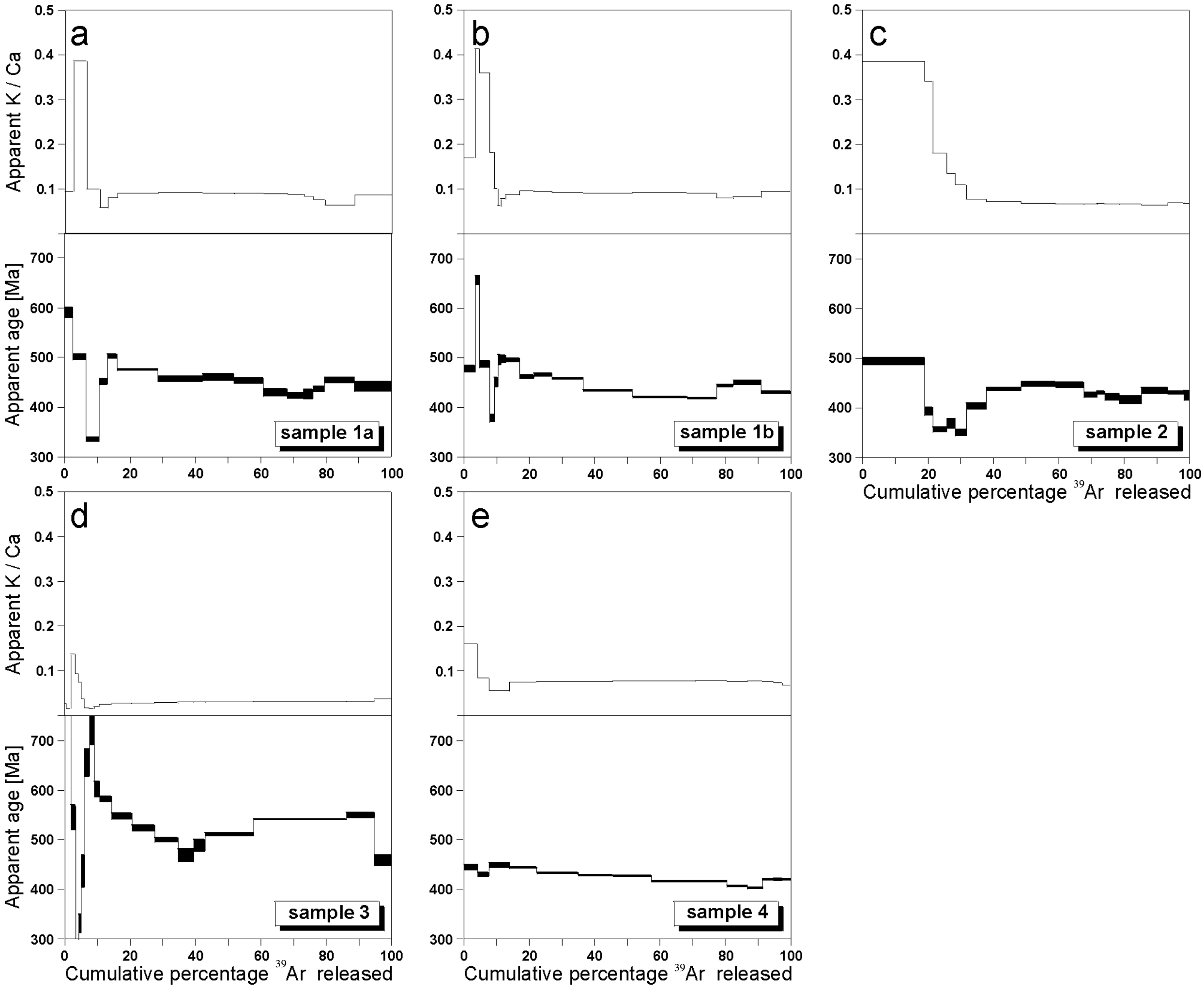

Fig. 3. ^{40}Ar/^{39}Ar apparent age and apparent K/Ca spectra of hornblende concentrates from the Kaintaleck Metamorphic Complex (locations shown in Figs. 1 and 2). Experimental temperatures increase from left to right. Analytical uncertainties (two sigma intralaboratory) are represented by vertical width of scale bars.

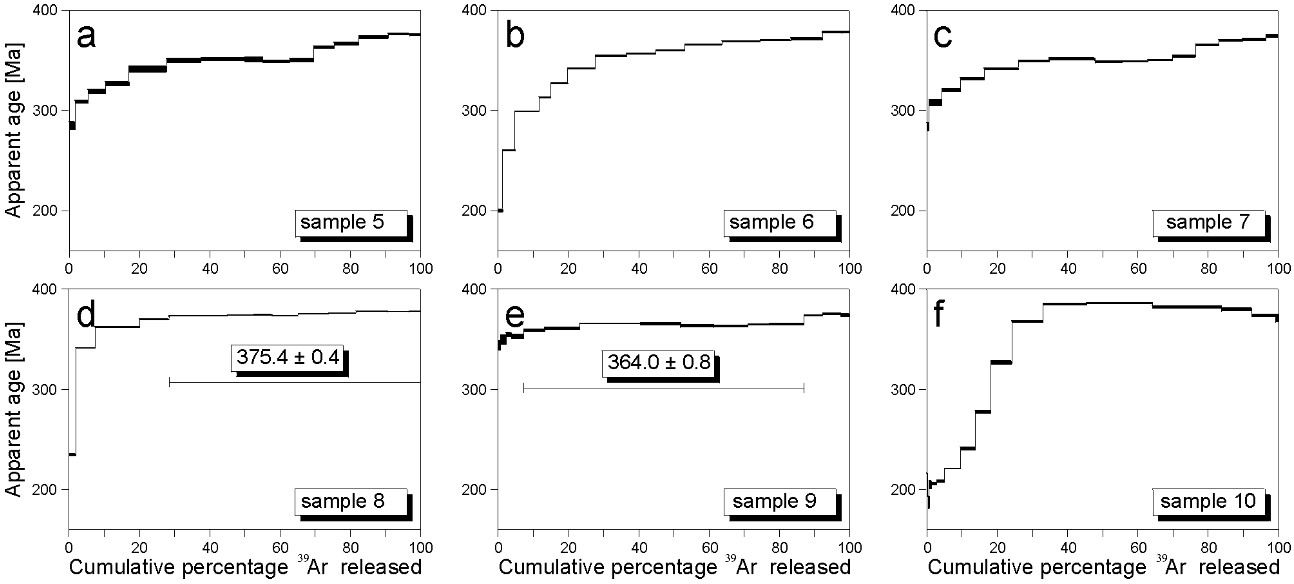

Fig. 4. ^{40}Ar/^{39}Ar apparent age spectra of white mica concentrates from the Kaintaleck Nappe (locations shown in Figs. 1 and 2). Data plotted as in Fig. 3. Plateau ages are listed and plateau increments are delineated.

Table 1: $^{40}Ar/^{39}Ar$ analytical data for incremental-heating experiments on hornblende samples from the Kaintaleck Nappe, Eastern Alps (Austria).

Release Temp. [°C]	$(^{40}Ar/^{39}Ar)^a$	$(^{36}Ar/^{39}Ar)^a$	$(^{37}Ar/^{39}Ar)^b$	^{39}Ar % of total	% ^{40}Ar non-atmos.^{c}	$^{36}Ar_{Ca}$ [%]	Apparent age [Ma]^d
Sample 1a (0.140-0.125 mm): J = 0.009878							
500	49.71	0.01866	0.124	0.01	74.06	0.08	559.6 ± 38.2
600	65.42	0.09062	5.432	2.55	59.72	1.63	590.6 ± 11.1
700	40.32	0.02700	1.340	4.01	80.47	1.35	501.9 ± 6.3
770	23.45	0.01082	5.150	4.08	88.11	12.95	336.0 ± 4.9
795	31.55	0.01202	8.774	2.41	90.96	19.85	452.5 ± 7.0
816	34.50	0.00870	6.334	2.98	94.01	19.80	503.1 ± 4.9
830	31.16	0.00381	5.680	12.45	97.83	40.57	476.3 ± 2.0
845	29.98	0.00431	5.622	13.66	97.24	35.48	457.9 ± 6.1
855	29.69	0.00258	5.705	9.74	98.95	60.10	461.1 ± 7.1
865	29.12	0.00249	5.710	8.90	99.03	62.49	453.6 ± 5.8
880	27.90	0.00406	5.728	7.25	97.33	39.42	430.1 ± 7.8
895	27.10	0.00287	5.824	5.06	98.58	55.24	423.8 ± 5.7
910	26.89	0.00168	6.154	2.88	99.98	99.84	426.4 ± 10.2
930	27.95	0.00290	6.779	3.53	98.86	63.48	437.0 ± 5.8
975	29.13	0.00290	8.018	9.07	99.25	75.24	455.3 ± 6.3
Fusion	28.30	0.00254	5.925	11.41	99.01	63.40	442.3 ± 10.3
Total	30.52	0.00707	5.872	100.00	95.98	47.76	454.1 ± 6.4
Sample 1b (0.160-0.140 mm): J = 0.008996							
600	51.68	0.06166	3.046	3.41	65.21	1.34	478.5 ± 7.6
700	59.34	0.03590	1.250	1.41	82.28	0.95	657.3 ± 10.1
770	41.11	0.02262	1.437	3.07	84.00	1.73	488.4 ± 7.1
795	29.89	0.01397	2.848	1.39	86.94	5.54	379.5 ± 8.4
815	35.10	0.01339	5.143	1.10	89.89	10.45	452.0 ± 10.2
870	37.54	0.01065	8.324	0.87	93.38	21.25	496.8 ± 10.6
890	36.89	0.00741	6.642	1.53	95.49	24.37	498.5 ± 7.8
905	35.40	0.00265	5.898	4.30	99.11	60.54	496.5 ± 4.1
920	32.94	0.00339	5.375	4.30	98.26	43.17	462.4 ± 4.0
935	33.09	0.00278	5.436	5.59	98.82	53.12	466.6 ± 3.5
950	32.44	0.00264	5.638	9.51	98.97	57.98	459.2 ± 1.9
965	30.56	0.00276	5.711	15.08	98.81	56.23	435.0 ± 2.4
980	29.39	0.00231	5.635	16.74	99.20	66.46	421.5 ± 1.8
1000	29.38	0.00292	5.699	8.96	98.60	53.07	419.1 ± 1.8
1030	31.62	0.00345	6.501	5.07	98.41	51.32	446.9 ± 3.1
1060	31.75	0.00263	6.296	8.62	99.13	65.10	451.3 ± 5.1
Fusion	30.58	0.00370	5.441	9.05	97.84	40.01	431.3 ± 2.7
Total	32.69	0.00632	5.441	100.00	96.59	50.00	448.1 ± 3.5
Sample 2: J = 0.009722							
620	36.74	0.01498	1.341	18.99	88.23	2.44	494.4 ± 7.7
720	30.46	0.01871	1.517	2.48	82.23	2.21	393.5 ± 8.2
770	26.06	0.01298	2.873	4.28	86.15	6.02	356.7 ± 5.6
795	24.88	0.00623	3.811	2.60	93.80	16.63	369.7 ± 10.3
810	24.56	0.00985	4.725	3.39	89.67	13.05	350.9 ± 7.1
825	26.94	0.00593	6.611	6.13	95.44	30.32	403.9 ± 6.2
840	28.81	0.00421	7.127	10.62	97.65	46.06	437.9 ± 3.8
855	29.36	0.00362	7.519	10.54	98.40	56.51	448.4 ± 5.4
865	29.29	0.00387	7.765	8.68	98.21	54.56	446.8 ± 5.5
880	28.70	0.00672	7.765	3.98	95.24	31.44	427.0 ± 6.0
895	27.80	0.00266	7.558	2.40	99.34	77.26	430.8 ± 3.5
910	27.19	0.00267	7.731	4.49	99.36	78.74	422.5 ± 7.1
925	27.40	0.00470	7.736	6.71	97.18	44.80	417.0 ± 8.2
960	28.31	0.00345	7.951	8.08	98.63	62.62	435.1 ± 6.6
1000	27.91	0.00277	7.417	4.85	99.18	72.82	431.6 ± 3.5
Fusion	28.37	0.00584	7.594	1.76	96.04	35.35	425.7 ± 10.3
Total	29.69	0.00717	5.797	100.00	94.72	37.96	435.7 ± 5.5
Sample 3: J = 0.009980							
675	362.09	0.38427	18.975	0.52	69.06	1.34	2273.3 ± 46.0
775	157.01	0.09693	31.995	1.29	83.39	8.98	1528.9 ± 15.3
825	44.39	0.03168	3.768	1.42	79.58	3.23	545.9 ± 25.5
845	22.27	0.02634	5.500	0.91	67.01	5.68	251.2 ± 15.0
865	26.30	0.02258	6.901	0.93	76.71	8.31	332.3 ± 18.8
890	33.93	0.02635	13.899	0.94	80.33	14.35	437.4 ± 33.1
920	50.23	0.03222	29.406	1.47	85.74	24.83	655.3 ± 28.5
940	52.92	0.21200	31.953	1.50	93.00	41.00	733.0 ± 42.9
960	47.73	0.03614	25.099	1.66	81.84	18.89	602.1 ± 15.9
980	40.90	0.01626	19.961	3.62	92.16	33.40	582.3 ± 5.6
1000	37.46	0.01297	18.630	6.30	93.75	39.06	547.6 ± 6.7
1020	35.73	0.01301	18.642	6.98	93.42	38.97	524.1 ± 6.5
1040	33.06	0.00963	17.815	7.11	95.70	50.30	499.9 ± 4.7
1060	30.56	0.00841	17.159	4.81	96.36	55.49	469.3 ± 12.8
1080	32.41	0.00992	17.247	3.39	95.22	47.30	489.1 ± 12.4
1100	33.89	0.00932	16.654	14.87	95.80	48.60	511.0 ± 3.3
1130	35.62	0.00761	16.434	28.40	97.38	58.72	541.2 ± 1.1
1170	37.02	0.01003	16.061	8.52	95.47	43.56	549.8 ± 5.5
Fusion	40.37	0.04306	14.015	5.36	71.25	8.85	458.9 ± 11.3
Total	39.36	0.01624	17.277	100.00	92.94	44.05	547.4 ± 7.1
Sample 4: J = 0.009565							
650	64.88	0.12144	3.236	4.19	45.08	0.72	445.8 ± 6.1
750	32.26	0.00609	6.138	3.45	94.10	27.40	430.7 ± 4.2
790	35.14	0.02180	9.310	6.26	83.78	11.62	449.9 ± 5.3
805	29.79	0.00425	6.897	8.37	97.63	44.17	444.5 ± 1.5
815	28.79	0.00357	6.720	12.77	98.19	51.17	433.4 ± 1.6
825	28.51	0.00373	6.752	10.37	98.01	49.19	429.0 ± 1.5
835	28.34	0.00334	6.655	12.07	98.39	54.25	428.0 ± 1.5
845	27.97	0.00436	6.678	13.29	97.30	41.70	418.9 ± 1.3
855	27.56	0.00340	6.608	9.67	98.26	52.79	417.0 ± 1.9
870	26.86	0.00348	6.773	6.28	98.18	52.94	407.3 ± 1.8
885	26.69	0.00376	6.695	4.51	97.83	48.42	403.7 ± 2.1
900	27.14	0.00537	6.831	3.55	96.15	34.60	403.5 ± 2.3
915	27.77	0.00340	7.069	2.66	98.40	56.48	420.6 ± 2.6
Fusion	28.02	0.00442	7.545	2.56	97.49	46.48	420.5 ± 2.4
Total	29.92	0.00995	6.746	100.00	94.67	43.66	423.0 ± 1.7

[a] measured

[b] corrected for post-irradiation decay of ^{37}Ar (35.1 day $^{1}/_{2}$ - life)

[c] $[^{40}Ar_{tot} - (^{36}Ar_{atmos}) \times (295.5)] / {}^{40}Ar_{tot}$

[d] calculated using correction factors of Dalrymple et al. (1981); two sigma, intralaboratory errors

polymetamorphic terrains to reflect partial rejuvenation of intracrystalline argon systems of white mica due to reheating and/or deformation induced recrystallization (e.g. Scaillet et al. 1990, 1992; Dallmeyer & Takasu 1992; West & Lux 1993). The internally discordant $^{40}Ar/^{39}Ar$ release spectra of garnet-micaschist samples 5, 6, and 7 are similar, and suggest initial isotopic closure for argon occurred prior to 375 Ma. Partial loss of radiogenic argon appears to have occurred during a greenschist-facies metamorphic overprint after initial closure of the isotopic system.

$^{40}Ar/^{39}Ar$ stepwise heating of muscovite from discordant aplitic gneiss sample 8 (Fig. 4d) yielded a well-defined plateau age of 375.4 ± 0.4 Ma in the 635 °C-fusion increments (together comprising 72 % of the ^{39}Ar released). A muscovite concentrate from discordant pegmatite sample 9 (Fig. 4e) yielded a well-defined plateau age of 364.0 ± 0.8 Ma in the 680–855 °C increments (together comprising 80 % of the total ^{39}Ar released). The apparent $^{40}Ar/^{39}Ar$ age spectra (Fig. 4d,e) display evidence for only minor loss of radiogenic ^{40}Ar subsequent to initial isotopic closure. These data are therefore considered geologically meaningful, and are interpreted as representing minimum estimates for the time of cooling subsequent to intrusion into previously deformed and metamorphosed garnet-micaschist and amphibolites.

Table 2: $^{40}Ar/^{39}Ar$ analytical data for incremental-heating experiments on muscovite samples from the Kaintaleck Nappe, Eastern Alps (Austria).

Release Temp. [°C]	$(^{40}Ar/^{39}Ar)^a$	$(^{36}Ar/^{39}Ar)^a$	$(^{37}Ar/^{39}Ar)^b$	^{39}Ar % of total	% ^{40}Ar non-atmos.^{c}	$^{36}Ar_{Ca}$ [%]	Apparent age [Ma]^d
Sample 5: J = 0.009363							
540	23.37	0.01716	0.061	1.68	78.29	0.10	285.2 ± 4.3
570	23.10	0.01062	0.006	3.72	86.39	0.02	309.0 ± 1.6
600	23.07	0.00806	0.005	4.93	89.66	0.02	319.2 ± 2.1
630	22.00	0.00260	0.005	6.70	96.49	0.05	326.9 ± 2.4
660	22.58	0.00106	0.005	10.62	98.59	0.13	341.4 ± 3.0
690	23.02	0.00042	0.005	9.82	99.43	0.29	350.2 ± 2.2
720	23.20	0.00077	0.005	12.51	98.99	0.18	351.3 ± 1.7
750	23.06	0.00030	0.007	5.04	99.59	0.61	351.3 ± 2.6
780	23.09	0.00090	0.004	7.76	98.83	0.13	349.2 ± 1.3
810	23.62	0.00240	0.005	6.71	96.97	0.05	350.4 ± 2.1
840	24.13	0.00095	0.005	5.85	98.81	0.13	363.4 ± 1.6
870	24.49	0.00134	0.008	7.03	98.36	0.17	366.8 ± 1.7
900	24.73	0.00054	0.007	8.39	99.33	0.36	373.4 ± 1.6
940	25.00	0.00066	0.007	6.05	99.20	0.31	376.5 ± 0.8
Fusion	24.86	0.00042	0.019	3.18	99.48	1.24	375.7 ± 1.1
Total	23.48	0.00200	0.007	100.00	97.43	0.22	350.0 ± 2.1
Sample 6: J = 0.009181							
500	14.11	0.00446	0.053	1.31	90.56	0.32	200.3 ± 1.6
580	17.97	0.00353	0.014	3.50	94.17	0.11	260.5 ± 0.8
610	19.87	0.00068	0.008	6.85	98.97	0.32	299.3 ± 0.4
640	20.94	0.00093	0.017	3.34	98.66	0.50	313.3 ± 1.0
670	21.88	0.00074	0.003	4.84	98.97	0.11	327.1 ± 0.6
700	23.01	0.00084	0.009	7.81	98.90	0.28	342.3 ± 0.6
730	23.93	0.00089	0.005	8.86	98.88	0.15	354.6 ± 0.8
760	24.05	0.00072	0.010	8.36	99.10	0.38	356.9 ± 0.4
790	24.25	0.00058	0.025	8.30	99.27	1.15	360.2 ± 0.6
820	24.67	0.00050	0.008	10.51	99.38	0.43	366.2 ± 0.6
850	24.87	0.00029	0.005	10.88	99.51	0.33	369.3 ± 0.6
880	24.90	0.00028	0.019	8.73	99.65	1.83	370.2 ± 0.6
910	25.10	0.00057	0.016	8.93	99.31	0.77	371.7 ± 1.4
945	25.48	0.00016	0.015	5.57	99.79	2.51	378.5 ± 0.8
Fusion	25.45	0.00060	0.020	2.20	99.91	9.14	378.5 ± 1.0
Total	23.57	0.00073	0.012	100.00	98.96	0.87	350.0 ± 0.7
Sample 7: J = 0.009996							
540	27.26	0.03447	0.021	0.63	62.62	0.02	284.2 ± 4.3
580	19.63	0.00340	0.003	3.67	94.86	0.02	307.9 ± 3.1
610	19.94	0.00165	0.003	5.26	97.53	0.05	320.5 ± 1.6
640	20.52	0.00107	0.004	6.74	98.44	0.10	331.8 ± 1.4
665	21.20	0.00113	0.003	9.81	98.40	0.06	341.8 ± 1.0
690	21.65	0.00092	0.003	8.64	90.72	0.09	349.4 ± 1.0
715	21.88	0.00116	0.005	13.05	98.40	0.11	351.7 ± 1.2
740	21.69	0.00115	0.003	7.80	98.40	0.07	348.9 ± 1.1
765	21.66	0.00096	0.005	7.30	98.66	0.13	349.3 ± 0.8
790	21.80	0.00113	0.005	6.96	98.44	0.11	350.5 ± 0.8
815	22.20	0.00162	0.003	6.58	97.82	0.04	354.4 ± 1.2
840	22.73	0.00084	0.004	6.60	98.89	0.12	365.6 ± 1.1
870	22.93	0.00047	0.003	6.71	99.36	0.16	370.1 ± 1.2
900	23.12	0.00086	0.004	6.70	98.88	0.13	371.3 ± 1.2
Fusion	23.20	0.00033	0.007	3.55	99.56	0.60	374.8 ± 1.5
Total	21.79	0.00134	0.004	100.00	98.19	0.11	349.5 ± 1.1
Sample 8: J = 0.010425							
480	16.71	0.01154	0.508	1.83	79.80	1.20	234.9 ± 1.3
560	20.91	0.00305	0.036	5.53	95.67	0.32	341.6 ± 0.5
585	21.52	0.00063	0.035	12.70	99.12	1.53	362.3 ± 0.6
610	21.94	0.00028	0.037	8.35	99.61	3.59	370.2 ± 0.6
635	22.12	0.00023	0.041	8.30	99.68	4.84	373.3 ± 0.3
660	22.21	0.00041	0.038	8.42	99.44	2.47	373.8 ± 0.3
685	22.29	0.00062	0.041	7.56	99.16	1.81	374.1 ± 0.4
715	22.28	0.00049	0.047	5.07	99.34	2.61	374.6 ± 0.5
740	22.29	0.00074	0.036	7.49	99.01	1.33	373.5 ± 0.2
770	22.36	0.00048	0.047	8.69	99.36	2.68	375.8 ± 0.3
800	22.48	0.00079	0.041	7.63	98.95	1.40	376.3 ± 0.5
835	22.59	0.00078	0.029	9.01	98.96	1.01	378.0 ± 0.4
870	22.59	0.00085	0.039	6.19	98.88	1.24	377.7 ± 0.2
Fusion	22.67	0.00103	0.041	3.23	98.65	1.10	378.0 ± 0.4
Total	22.04	0.00092	0.047	100.00	98.66	2.05	368.8 ± 0.4
Total without 480 ° – 610 °C				71.59			375.4 ± 0.4
Sample 9: J = 0.009738							
550	46.47	0.08424	0.028	0.68	46.42	0.01	344.0 ± 5.1
590	28.38	0.02164	0.004	1.61	77.44	0.01	349.8 ± 4.6
625	23.65	0.00449	0.020	1.46	94.38	0.12	354.9 ± 2.1
650	22.94	0.00248	0.004	3.54	96.78	0.04	353.1 ± 2.3
680	22.73	0.00042	0.003	5.90	99.43	0.21	358.9 ± 1.3
705	22.84	0.00027	0.003	9.96	99.63	0.28	361.0 ± 1.1
730	23.19	0.00034	0.003	17.30	99.54	0.25	365.9 ± 0.7
755	23.13	0.00017	0.003	11.43	99.76	0.51	365.7 ± 1.4
780	22.97	0.00013	0.004	9.39	99.81	0.80	363.6 ± 1.5
805	23.02	0.00039	0.003	9.77	99.48	0.22	363.1 ± 1.0
830	23.16	0.00043	0.004	6.13	99.43	0.26	365.0 ± 0.8
855	23.41	0.00125	0.003	9.88	98.40	0.06	365.2 ± 0.8
885	23.71	0.00021	0.003	5.31	99.72	0.43	373.9 ± 0.9
920	23.86	0.00032	0.003	5.10	99.58	0.26	375.5 ± 1.2
Fusion	23.87	0.00060	0.006	2.53	99.23	0.26	374.3 ± 1.5
Total	23.42	0.00145	0.004	100.00	98.58	0.31	364.5 ± 1.0
Total without 550 ° – 650 °C, 885 °C - fusion				79.76			364.0 ± 0.8
Sample 10: J = 0.009892							
550	25.89	0.04608	1.718	0.26	47.91	1.01	208.9 ± 8.1
550	15.11	0.01380	0.394	0.35	73.18	0.78	187.2 ± 6.2
600	13.17	0.00408	2.366	0.67	92.26	15.79	205.1 ± 4.1
650	12.68	0.00186	1.327	1.48	96.47	19.44	206.1 ± 1.4
690	12.75	0.00136	0.575	2.23	97.17	11.52	208.6 ± 1.3
730	13.41	0.00088	0.457	4.43	98.29	14.14	221.1 ± 0.6
760	14.59	0.00049	0.226	4.26	99.10	12.66	241.1 ± 1.8
790	17.06	0.00075	0.162	4.53	98.74	5.86	277.9 ± 1.6
815	20.23	0.00050	0.302	5.92	99.36	16.55	327.1 ± 1.9
840	22.95	0.00039	0.272	8.92	99.57	19.22	367.7 ± 1.2
865	24.11	0.00026	0.340	12.42	99.77	35.27	385.1 ± 1.0
895	24.21	0.00028	0.275	18.62	99.72	26.59	386.4 ± 0.8
925	23.91	0.00016	0.206	19.67	99.85	35.19	382.5 ± 1.2
955	23.73	0.00018	0.324	8.65	99.86	48.55	379.9 ± 1.8
990	23.34	0.00027	0.287	6.71	99.73	28.81	373.8 ± 1.2
Fusion	22.94	0.00002	1.839	0.88	100.59	2363.54	371.3 ± 4.1
Total	21.94	0.00056	0.331	100.00	99.22	47.96	351.3 ± 1.9

[a] measured

[b] corrected for post-irradiation decay of ^{37}Ar (35.1 day $^{1}/_{2}$ - life)

[c] $\left[{}^{40}Ar_{tot} - ({}^{36}Ar_{atmos}) \times (295.5)\right] / {}^{40}Ar_{tot}$

[d] calculated using correction factors of Dalrymple et al. (1981); two sigma, intralaboratory errors

The $^{40}Ar/^{39}Ar$ release spectra of a muscovite concentrate (sample 10) separated from an orthogneiss boulder within the Kalwang Conglomerate (locality near Bruck a.d. Mur) is displayed in Fig. 4f. In contrast to the white mica analyses discussed above, the K/Ca ratios of this sample are much lower (Table 2), but again no significant variation and correlation with the $^{40}Ar/^{39}Ar$ ratios is visible. The argon release spectra of this sample is disturbed, which might reflect either partial isotopic resetting and/or mixing of different white mica phases with distinct ages. However, intermediate- and high-temperature gas release ages of up to 385 Ma reported in this spectrum are interpreted as representing minimum ages for cooling following metamorphism of the source area prior to erosion and deposition of this conglomerate.

Discussion

The new geochronological results demonstrate that Alpine greenschist-facies metamorphism and accompanied penetrative ductile deformation did not completely reset $^{40}Ar/^{39}Ar$ isotopic systems in hornblende and white mica of amphibolite-facies metamorphic basement rocks. Alpine $^{40}Ar/^{39}Ar$ apparent ages are not recorded even in low-temperature portions of the white mica analyses. The relatively low Alpine overprint allows resolution of the chronology of the pre-Alpine tectonothermal history of the Kaintaleck Nappe. The isotopic data demonstrate that amphibolite-facies metamorphic conditions were reached prior to ca. 400 Ma (Early Devonian according to time-scale calibration of Harland et al. 1990), as indicated by youngest ages reported in medium- and high-temperature release steps of hornblende. Ages of ca. 375 Ma are reported in medium- and high-temperature gas fractions evolved during incremental Ar-heating analyses of white micas from garnet-micaschist. Evidence for an early Devonian tectonometamorphic event is also reflected by results from croscutting pegmatites and aplitic veins, for which $^{40}Ar/^{39}Ar$ plateau ages of 364.0 ± 0.8 Ma (pegmatite sample 9) and 375.4 ± 0.4 Ma (aplitic gneiss sample 8) are recorded. Additional evidence comes from an orthogneiss boulder within the transgressive Kalwang Conglomerate, for which maximum apparent $^{40}Ar/^{39}Ar$ ages of ca. 385 Ma are recorded in medium- and high-temperature increments. These indicate the age of cooling prior to erosion and deposition of the respective source area. As suggested by U-Pb zircon data and high-pressure relics in eclogitic garnet-amphibolite, this Devonian cooling could have been preceded by a higher grade metamorphism (Neubauer & Frisch 1993).

Tectonic implications

The Devonian post-metamorphic cooling ages presented in this study suggest that the Kaintaleck Metamorphic Complex and its low-grade metamorphic cover (e.g. the Kalwang Conglomerate) do not represent the basement for Ordovician clastic sequences of the Noric-Tirolic nappe complex as suggested by Daurer & Schönlaub (1978) and Neubauer et al. (1987). By contrast, the Kaintaleck Nappe appears to represent an individual tectonic unit which was incorporated into the Upper Austroalpine nappe complex during early Alpine thrusting, as indicated by $^{40}Ar/^{39}Ar$ plateau ages of ca. 98–94 Ma reported for white mica and whole-rock samples from penetrative deformed phyllite and mylonite in footwall and hangingwall structural units (Dallmeyer et al. 1998). Devonian cooling ages have been reported for detrital white mica from Permian clastic sequences of the Silbersberg Nappe (footwall of the Kaintaleck Nappe, Fig. 2) and may suggest a pre-Alpine association of the Kaintaleck Metamorphic Complex with sedimentary units of the Silbersberg Nappe (Handler et al. 1997).

Devonian tectonothermal evolution contrasts with the regional Paleozoic evolution of basement units within other structural units of the Austroalpine nappe complex. These typically record the effects of upper greenschist- and amphibolite-facies metamorphism at ca. 300–330 Ma (Frank et al. 1987). However, mineral cooling ages related to Devonian metamorphism have been reported from several other base-

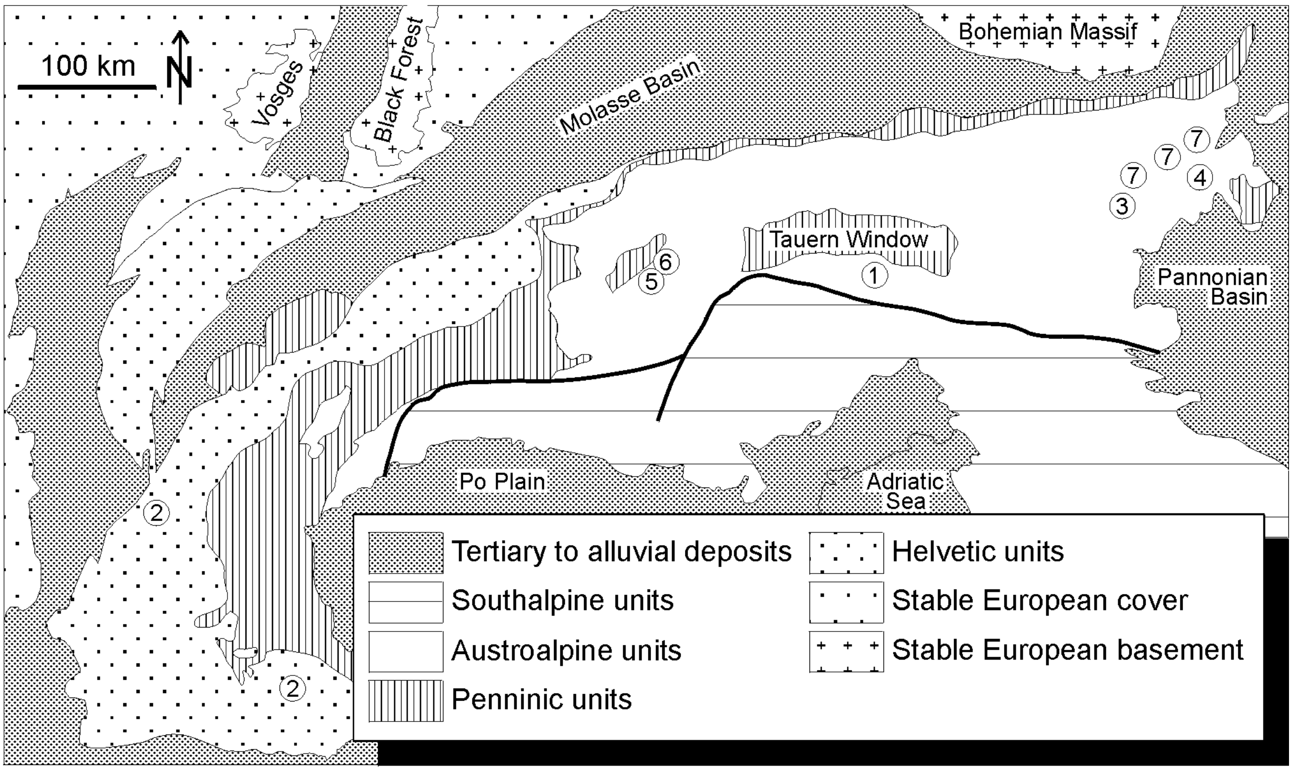

Fig. 5. Geological sketch map of the Alps indicating locations of Silurian–Devonian mineral cooling ages ranging between 440 and 380 Ma. (1) Cliff 1980, (2) Paquette et al. 1989, (3) Neubauer & Frisch 1993, (4) Müller et al. 1999, (5) Schweigl 1995, (6) Hoinkes et al. 1997, (7) this study.

ment units of the Alpine orogen (Fig. 5). These include Devonian white mica cooling ages from western sectors of the Middle Austroalpine nappe complex (Lichem 1993; Schweigl 1995; Hoinkes et al.1997) and eastern sectors of the Lower Austroalpine nappe complex within the Eastern Alps (Müller et al. 1999). The latter have been interpreted to date initial high-pressure metamorphism. Additional U-Pb zircon data indicating Devonian high-pressure metamorphism within the Austroalpine basement have been reported by Cliff (1980) and Neubauer & Frisch (1993). Frisch & Neubauer (1989) defined the Wechsel, Pannonic, and Veitsch tectonostratigraphic subdivisions of the Austroalpine basement and suggested these are characterized by Devonian deformation and metamorphism. Silurian-Devonian high-pressure metamorphism has also been reported from the Helvetic basement units in the External Massifs of the Central Alps (Paquette et al. 1989). Largescale correlation of pre-Alpine basement units has been carried out by Flügel (1990), Frisch et al. (1990), Neubauer & von Raumer (1993), and von Raumer & Neubauer (1993). These authors suggest linkages of Devonian metamorphic basement units within the Alpine belt to the Ligerian Cordillera (Matte 1986) of the southern Armorican Massif and the Moldanubian Zone of the Bohemian Massif. Therefore the Kaintaleck Metamorphic Complex may represent a fragment of the Ligerian Cordillera which was deformed and metamorphosed during its Devonian accretion to stable Europe. It partly rifted from stable Europe during Permian to Jurassic extension and was finally accreted to Europe again during the Alpine orogenic events.

Acknowledgments: This research was supported, in part, by a grant from the Tectonics Program of the U.S. National Science Foundation (EAR-9316042) to R.D.D. and the Austrian Research Foundation (P 7405-GEO and P 8652-GEO) to F.N. R.H. acknowledges grants from the Austrian Research Community and Austrian Government for a three-months visit at R.D.D.'s K-Ar laboratory.

Appendix

Topographic names are from the 1:50,000 Austrian topographic maps (ÖK 50). For more information on the geological situation at each sampling site we refer to Neubauer et al. 1994 and references therein.

Sample 1: Location: ÖK 133 sheet Leoben; south of Oberdorf in the Laming Valley on the mountain slope east of the Obertalergraben; roadcut on gravel road which connects the farmers Leber and Wieser with the gravel road which leads from Oberdorf to the Tulleralm; approximately 50 m south of the intersection; altitude 850 m: Medium grained amphibolite with weakly developed foliation and mineral lineation; the amhibolite suffered minor alteration under greenschist facies metamorphic conditions; old amphiboles and feldspars are surrounded by a new grown, fine-grained matrix of carbonate, Mg-rich chlorite, epidote, zoisite/clinozoisite, titanite and ilmenite, best developed along discrete shear bands.

Sample 2: Location: ÖK 133 sheet Leoben; Tanzenberg tunnel on highway S6 east of Bruck a.d. Mur; bore hole-meter 112.3: Coarse-grained, strongly deformed garnet-amphibolite; garnets and amphiboles belong to the old mineral assemblage and suffered external rotation into the new developed foliation, garnets are almost completely cracked, amphiboles are oriented parallel to the stretching lineation; the new grown matrix consists of mineral phases typical for greenschist metamorphic overprinting of amphibolites such as epidote, zoisite, clinozoisite, carbonate, quartz, titanite, ilmenite and Fe-rich chlorite.

Sample 3: Location: ÖK 133 sheet Leoben; Tanzenberg tunnel on highway S6 east of Bruck a.d. Mur; ca. 500 m south-west of the Tanzenberg: Amphibolite of the Ritting structural subunit; the sample mainly consists of large amphibole crystals, garnet and zoisite; elongated zoisite crystals display a shape preferred parallel orientation; garnet is often surrounded by symplectite which is composed of fine-grained quartz, albite, and fine-grained amphibole; large amphibole crystals are internally unzoned; secondary deformation is low and expressed in minor kinking of some amphibole grains.

Sample 4: Location: ÖK 104 sheet Müzzuschlag; southwest of Neuberg a.d. Mürz, on top of the ridge east of the Arzbachhöhe; altitude 870 m: Less foliated fine-grained amphibolite; amphiboles show no preferred orientation within a matrix of feldspar, partly altered to sericite, epidote, zoisite, and titanite.

Sample 5: Location: ÖK 133 sheet Leoben; south of Oberdorf in the Laming Valley on the mountain slope east of the Obertalergraben; roadcut on gravel road which connects the farmers Leber and Wieser with the gravel road which leads from Oberdorf to the Tulleralm; approximately 60 m south of the intersection and 10 m in the footwall of sample 1; altitude 850 m: Grayish-brown, medium grained garnet-micaschist with well developed foliation; white micas are oriented parallel to the foliation, quartz exhibits core-mantle-textures with only minor recrystallization; garnet shows brittle deformation, fractures are filled with new grown Fe-rich chlorite.

Sample 6: Location: ÖK 105 sheet Neunkirchen; on top of the mountain ridge above the railway station at Schlögelmühl; altitude 570 m: Grayish-brown, medium grained garnet-micaschist with well developed foliation and cataclastic texture; old quartz grains shows core-mantle textures and undulatory extinction, feldspars are decomposed to sericite and quartz, garnets show extreme elongation due to brittle deformation, their cracks are filled with chlorite, white micas suffered external rotation into the foliation; the new grown matrix is build up by fine grains quartz, sericite, chlorite and ilmenite.

Sample 7: Location: ÖK 133 sheet Leoben; south of Oberdorf in the Laming Valley, on the mountain slope west of the Obertalergraben; roadcut on gravel road 620 m east of the farmer Maxl; altitude 960 m: Greenish-gray, fine-grained micaschist with well developed foliation; white micas up to 2 mm in diameter are oriented parallel to the stretching lineation; components are quartz, clasts of feldspar and white mica and minor epidote and zoisite.

Sample 8: Location: ÖK 105 sheet Neunkirchen; roadcut on the road from Pottschach to Vöstenhof, 100 m south of the castle Vöstenhof; altitude 500 m: White aplitic gneiss with well developed ductile foliation and mineral stretching lineation; quartz is characterized by the development of elongated grains with subgrain formation, feldspars, almost only plagioclase, shows strong retrogressive metamorphic overprint and sericitization.

Sample 9: Location: ÖK 133 sheet Leoben; 550 m NNW of the chapel in the village Laintal III; altitude 905 m: Coarse-grained, unfoliated white pegmatite; dominant constituents are plagioclase (partly decomposed to sericite), quartz, white micas, up to 4 cm in diameter and 5 mm thickness, and minor garnet.

Sample 10: Location: ÖK 134 sheet Passail; small exposure within the forest above the farm Schwammberger north of the village Frauenberg, east of Bruck a.d. Mur; altitude 910 m: Orthogneiss boulder within the Kalwang Conglomerate; elongated grains of undulose quartz, albite, and minor K-feldspar form the foliation; quartz shows low-angle grain boundaries and fine recrystallized grains along margins of older grains; a few grains of internally zoned garnets occur along grain boundaries of quartz and plagioclase or as inclusions within quartz; muscovite forms flakes which are affected by microboudinage and minor recrystallization to fine-grained sericite along margins of larger flakes.

References

Barber D.J., 1985: Dislocations and microstructures. In: Wenk H.R. (Ed.): *Preferred orientation in deformed metals and rocks: An introduction to modern texture analysis. Academic Press,* Orlando–New York–London, 149–182.

Bell T.H. & Etheridge M.A., 1973: Microstructure of mylonites and their descriptive terminology. *Lithos,* 6, 337–348.

Cliff R.A., 1980: U-Pb isotopic evidence from zircons for lower Paleozoic tectonic activity in the Austroalpine nappe, the Eastern Alps. *Contr. Mineral. Petrology,* 71, 283–288.

Coward M.P. & Dietrich D., 1989: Alpine tectonics — an overview. In: Coward M.P., Dietrich D. & Park R.G. (Eds.): *Alpine Tectonics. Geol. Soc. Spec. Publ.,* 45, 1–29.

Dallmeyer R.D. & Gil Ibargurchi J.I., 1990: Age of amphibolitic metamorphism in the ophiolitic unit of the Morais allochthon (Portugal): Implications for early Hercynian Orogenesis in the Iberian Massif. *J. Geol. Soc., (London)*, 147, 873–878.

Dallmeyer R.D. & Keppie J.D., 1987: Polyphase late Paleozoic tectonothermal evolution of the southwestern Meguma Terrane, Nova Scotia: Evidence from $^{40}\mathrm{Ar}/^{39}\mathrm{Ar}$ mineral ages. *Canad. J. Earth Sci.,* 24, 1242–1254.

Dallmeyer R.D. & Takasu A., 1992: $^{40}\mathrm{Ar}/^{39}\mathrm{Ar}$ ages of detrital muscovite and whole-rock slate/phyllite, Narragansett Basin, RI-MA, USA: Implications for rejuvenation during very low-grade metamorphism. *Contr. Mineral. Petrology*, 110, 515–527.

Dallmeyer R.D., Neubauer F., Handler R., Fritz H., Müller W., Pana D. & Putiš M., 1996: Tectonothermal evolution of the internal Alps and Carpathians: Evidence from $^{40}\mathrm{Ar}/^{39}\mathrm{Ar}$ mineral and whole-rock data. *Eclogae Geol. Helv.,* 89, 203–227.

Dallmeyer R.D., Handler R., Neubauer F. & Fritz H., 1998: Sequence of thrusting within a thick-skinned tectonic wedge: Evidence from $^{40}\mathrm{Ar}/^{39}\mathrm{Ar}$ and Rb-Sr ages from the Austroalpine nappe complex of the Eastern Alps. *J. Geol.,* 106, 71–86.

Dalrymple G.B., Alexander E.C., Lanphere M.A. & Kraker G.P., 1981: Irradition of samples of $^{40}\mathrm{Ar}/^{39}\mathrm{Ar}$ dating using the Geological Survey TRIGA reactor. *U.S. Geol. Surv. Prof. Pap.*, 1176, 1–55.

Daurer A. & Schönlaub H.P., 1978: Anmerkungen zur Basis der Nördlichen Grauwackenzone. *Mitt. Österr. Geol. Gesell.,* 69, 77–88.

Den Brok B., 1992: An experimental investigation into the effect of water on the flow of quartzite. *Geologica Ultraiect.,* 95, 1–178.

Dewey J.F., Helmann M.L., Turco E., Hutton D.H.W. & Knott S.D., 1989: Kinematics of the Western Mediterranean. In: Coward M.P., Dietrich D. & Park R.G. (Eds.): *Alpine Tectonics. Geol. Soc. Spec. Publ.*, 45, 265–283.

Etheridge M.A. & Wilkie J.C., 1979: Grainsize reduction, grain boundary sliding and the flow strength of mylonites. *Tectonophysics,* 58, 159–178.

Etheridge M.A. & Wilkie J.C., 1981: An assessment of dynamically recrystallized grainsize as a paleopiezometer in quartz-bearing mylonite zones. *Tectonophysics,* 78, 475–508.

Flügel H.W., 1990: Das voralpine Basement im Alpin-Mediterranen Belt—Übersicht und Problematik. *Jb. Geol. Bundesanst.*, 133, 181–221.

Frank W., 1987: Evolution of the Austroalpine elements in the Cretaceous. In: Flügel H.W. & Faupl P. (Eds.): *Geodynamics of the Eastern Alps. Deuticke*, Vienna, 379–406.

Frank W., Kralik M., Scharbert S. & Thöni M., 1987: Geochronological data from the Eastern Alps. In: Flügel H.W. & Faupl P. (Eds.): *Geodynamics of the Eastern Alps. Deuticke*. Vienna, 272–281.

Frisch W., 1979: The plate tectonic evolution of the Alps. *Tectonophysics*, 60, 121–134.

Frisch W. & Neubauer F., 1989: Pre-Alpine terranes and tectonic zoning in the Eastern Alps. In: Dallmeyer R.D. (Ed.): *Terranes in the Circum-Atlantic Paleozoic Orogens. Geol. Soc. Amer. Spec. Pap.*, 230, 91–100.

Frisch W., Neubauer F. & Satir M., 1984: Concepts of the evolution of the Austroalpine basement complex (Eastern Alps) during the Caledonian-Variscan cycle. *Geol. Rdsch.*, 73, 47–68.

Frisch W., Menot R.P., Neubauer F. & von Raumer J., 1990: Correlation and evolution of the Alpine basement. *Schweiz. Mineral. Petrogr. Mitt.,* 70, 265–285.

Gebauer D., 1993: The pre-Alpine evolution of continental crust of the central Alps—An overview. In: von Raumer J. & Neubauer F. (Eds.): *Pre-Mesozoic geology in the Alps. Springer*, Berlin-Heidelberg–New York, 94–117.

Gottstein G. & Mecking H., 1985: Recrystallization. In: Wenk H.R. (Ed.): *Preferred orientation in deformed metals and rocks: An introduction to modern texture analysis. Academic Press,* Orlando–New York–London, 183–218.

Handler R., 1994: $^{40}\mathrm{Ar}/^{39}\mathrm{Ar}$ and Rb-Sr mineral dating within a complex polymetamorphic terrain: The northeastern Alps, Austria. *Ph. D. Thesis,* Graz, 1–143.

Handler R., Dallmeyer R.D. & Neubauer F., 1997: $^{40}\mathrm{Ar}/^{39}\mathrm{Ar}$ ages of detrital white mica from Upper Austroalpine units in the Eastern Alps, Austria: Evidence for Cadomian and contrasting Variscan sources. *Geol. Rdsch.*, 86, 69–80.

Harland W.B., Armstrong R.L., Cox A.V., Craig L.E., Smith A.G. & Smith D.G., 1990: A geologic time scale 1989. *Cambridge University Press*, Cambridge, 1–263.

Hoinkes G. & Thöni M., 1993: Evolution of the Ötztal-Stubai, Scarl-Campo and Ulten Basement Units. In: von Raumer J. & Neubauer F. (Eds.): *Pre-Mesozoic geology in the Alps. Springer*, Berlin-Heidelberg-New York, 485–494.

Hoinkes G., Thöni M., Lichem C., Berhard F., Kaindl R., Schweigl J., Tropper P. & Cosca M., 1997: Metagranitoids and associated metasediments as indicators for the pre-Alpine magmatic and metamorphic evolution of the western Austroalpine Ötztal Basement (Kaunertal, Tirol). *Schweiz. Mineral. Petrogr. Mitt.*, 77, 299–314.

Kralik M., Krumm H. & Schramm J.M., 1987: Low grade and very low grade metamorphism in the Northern Calcareous Alps and in the Greywacke zone: Illite-crystallinity data and isotopic ages. In: Flügel H.W. & Faupl P. (Eds.): *Geodynamics of the Eastern Alps. Deuticke*, Vienna, 164–178.

Langdon T.G., 1985: Regimes of plastic deformation. In: Wenk H.R. (Ed.): *Preferred orientation in deformed metals and rocks: An introduction to modern texture analysis. Academic Press,* Orlando–New York–London, 219–232.

Lichem C., 1993: Petrologische und geochemische Untersuchungen an Orthogneissen des westlichen Ötztal-Stubai Kristallins (Kaunertal). *M. Sci. Thesis*, Graz, 1–139.

Lister G.S. & Snoke A.W., 1984: S-C Mylonites. *J. Struct. Geol.*, 6, 617–638.

Loeschke J., Kretzschmar T., Langer V. & Streck M., 1990: Zur Geologie der Norischen Decke nordwestlich von Kalwang (Eisenerzen Alpen, Steirische Grauwackenzone/Österreich). *Jb. Geol. Bundesanstal.*, 133, 345–363.

Maggetti M. & Flisch M., 1993: Evolution of the Silvretta Nappe. In: von Raumer J. & Neubauer F. (Eds.): *Pre-Mesozoic geology in the Alps. Springer*, Berlin-Heidelberg–New York, 469–484.

Matte P., 1986: Tectonics and plate tectonics model for the Variscan belt of Europe. *Tectonophysics*, 126, 329-374.

Müller W., Dallmeyer R.D., Neubauer F. & Thöni M., 1999: Deformation-induced resetting of Rb/Sr and ^{40}Ar/^{39}Ar mineral systems in a low-grade, polymetamorphic terrane (Eastern Alps, Austria). *J. Geol. Soc.*, *(London)*, 156, 261-278.

Neubauer F., 1985: Eine prä-oberordovizische Transgression in der Grauwackenzone (Ostalpen) und ihre Bedeutung für paläozoische Geodynamik und alpinischen Deckenbau. *N. Jb. Geol. Paläont. Mh.,* 1985, 46-64.

Neubauer F. & Frisch W., 1993: The Austro-Alpine metamorphic basement East of the Tauern Window. In: von Raumer J. & Neubauer F. (Eds.): *Pre-Mesozoic geology in the Alps. Springer*, Berlin-Heidelberg-New York, 515-536.

Neubauer F. & von Raumer J., 1993: The alpine basement-linkage between Variscides and East-Mediterranean Mountain Belts. In: von Raumer J. & Neubauer F. (Eds.): *Pre-Mesozoic geology in the Alps. Springer*, Berlin-Heidelberg-New York, 641-663.

Neubauer F., Frisch W. & Hansen B.T., 1987: Time relation between Eoalpine metamorphism and thrusting: Evidence from the crystalline basement of the eastern Greywacke Zone. In: Flügel H.W. & Faupl P. (Eds.): *Geodynamics of the Eastern Alps. Deuticke*, Vienna, 263-271.

Neubauer F., Handler R., Hermann S. & Paulus G., 1994: Revised lithostratigraphy and structure of the Eastern Graywacke Zone (Eastern Alps). *Mitt. Österr. Geol. Gesell.,* 86, 61-74.

Paquette J.L., Menot R.P. & Peucot J.J., 1989: REE, Sm-Nd and U-Pb zircon study of eclogites from the Alpine External Massif (Western Alps): Evidence for crustal contamination. *Earth Planet. Sci. Lett.*, 96, 181-198.

Samson S.D. & Alexander E.C., 1987: Calibration of the interlaboratory ^{40}Ar/^{39}Ar dating standard, Mmhb-1. *Chem. Geol. (Isot. Geosci. Sect.),* 66, 27-34.

Scaillet S., Féraud G., Lagabrielle Y., Ballévre M. & Ruffet G., 1990: ^{40}Ar/^{39}Ar laser-probe dating by step heating and spot fusion of phengites from the Dora Maira Nappe of the western Alps, Italy. *Geology,* 18, 741-744.

Scaillet S., Féraud G., Ballévre M. & Amouric M., 1992: Mg/Fe and [(Mg, Fe) Si-Al$_2$] compositional control on argon behaviour in high-pressure white micas: A ^{40}Ar/^{39}Ar continuous laser-probe study from the Dora-Maira Nappe of the internal western Alps, Italy. *Geochim. Cosmochim. Acta*, 56, 2851-2872.

Schmid S.M., 1982: Microfabric studies as indicators of deformation mechanism and flow laws operative in mountain building. In: Hsü K.J. (Ed.): *Mountain building processes. Academic Press*, London, 95-110.

Schulz B., Nollau G., Heinisch H. & Godizart G., 1993: Austro-Alpine basement complex to the south of the Tauern Window. In: von Raumer J. & Neubauer F. (Eds.): *Pre-Mesozoic geology in the Alps. Springer*, Berlin-Heidelberg-New York, 495-514.

Schweigl J., 1995: Neue geochronologische und isotopengeologische daten zur voralpidischen Entwicklungsgeschichte im Ötztalkristallin (Ostalpen). *Jb. Geol. Bundesanst.*, 138, 131-149.

Sibson R.H., 1977: fault rocks and fault mechanisms. *J. Geol. Soc., (London)*, 133, 191-213.

Sibson R.H., 1980: Transient discontinuities in ductile shear zones. *J. Struct. Geol.*, 2, 165-171.

Spillmann P. & Büchi H., 1993: The pre-Alpine basement of the Lower Austro-Alpine nappes in the Bernina Massif (Grisons, Switzerland; Valtellina, Italy). In: von Raumer J. & Neubauer F. (Eds.): *Pre-Mesozoic geology in the Alps. Springer*, Berlin-Heidelberg-New York, 457-467.

Steiger R.H. & Jäger E., 1977: Subcommission on geochronology: Convention on the use of decay constants in geo- and comsochronology. *Earth Planet. Sci. Lett.*, 36, 359-362.

Thöni M. & Jagoutz E., 1993: Isotopic constraints for eo-Alpine high-P metamorphism in the Austroalpine nappes of the Eastern Alps: Bearing on Alpine orogenesis. *Schweiz. Mineral. Petrogr. Mitt.*, 73, 177-189.

Tollmann A., 1963: Ostalpensynthese. *Deuticke*, Vienna, 1-256.

Tollmann A., 1987: The Alpidic evolution of the eastern Alps. In: Flügel H.W. & Faupl P. (Eds.): *Geodynamics of the Eastern Alps. Deuticke*, Vienna, 361-378.

von Raumer J. & Neubauer F., 1993: Late Precambrian and Paleozoic evolution of the Alpine basement—An Overview. In: von Raumer J. & Neubauer F. (Eds.): *Pre-Mesozoic geology in the Alps. Springer*, Berlin-Heidelberg-New York, 625-639.

West D.P.Jr. & Lux D.R., 1993: Dating mylonitic deformation by the ^{40}Ar/^{39}Ar method: An example from the Norumbega Fault Zone, Main. *Earth Planet. Sci. Lett.*, 120, 221-237.

White S.H., 1976: The effects of strain on microstructures, fabrics, and deformation mechanism in quartzites. *Phil. Trans. R. Soc., (London),* A283, 69-86.

White S.H., 1977: Geological significance of recovery and recrystallization processes in quartz. *Tectonophysics,* 39, 143-170.